Numerical simulations of quantum two-dimensional Heisenberg ferromagnetics

1992 J. Phys.: Condens. Matter 4 2629

(http://iopscience.iop.org/0953-8984/4/10/025)

J. Phys.: Condens. Matter 4 (1992) 2629–2640. Printed in the UK

Numerical simulations of quantum two-dimensional Heisenberg ferromagnetics

I A Favorsky, T V Kuznetsova and P N Vorontsov-Velyaminov
Scientific Research Institute of Physics, St Petersburg State University, 198904, Stary Peterhoff, St Petersburg, Russia

Received 15 May 1991

Abstract. Quantum two-dimensional Heisenberg ferromagnetic systems were studied using the Handscomb Monte Carlo approach. Temperatures ranged from 0.3 to 4.0 J. The large system sizes used made it possible to apply scaling methods and to calculate infinite system susceptibility values for temperatures considerably lower than have been studied elsewhere. The internal energy was found to be essentially size-independent for all temperatures. Comparisons were drawn between the Godfrin *et al* experimental observation of the quantum two-dimensional ferromagnetism in thin films of ^{3}He and our results for temperature dependence of simulated susceptibility. The existence of several essential similarities was verified; for example, the non-exponential low-temperature behaviour of χT. Our results for susceptibility and energy were compared with other numerical simulations and various theoretical predictions. The comparisons have enabled us to define temperature regions where high and low temperature approximations are valid. Monte Carlo results also fill the gap between the approximations.

1. Introduction

Quantum two-dimensional magnetic systems have been receiving considerable attention for some time now. The discovery of high-temperature superconductivity stimulated an interest in Heisenberg antiferromagnetism, since two-dimensional antiferromagnetic subsystems were found in La_2CuO_4 [1, 2]. The experimental observation of quantum ferromagnetism in thin films of ^{3}He was reported recently by Godfrin *et al* [3].

In the present work we have applied the so-called Handscomb quantum Monte Carlo (MC) method [4] to study the two-dimensional quantum Heisenberg ferromagnetic model. The Handscomb method, as was first noticed by Lyklema [5], runs into serious difficulties when applied to the antiferromagnetic case. Although it is the latter that is of special importance to superconductivity theory, it is possible that the functional forms of observables such as energy, susceptibility and correlation length are essentially the same for both types of magnetization.

The existing theories of quantum Heisenberg magnetics [1, 2, 6–8] frequently disagree with each other; their regions of applicability are sometimes uncertain, and some of the theories substitute classical vectors for quantum spins. The numerical simulations made it possible for us to clarify some of the problems mentioned.

0953-8984/92/102629 + 12 $04.50

We have used the Handscomb Monte Carlo approach to study the thermodynamical properties of the two-dimensional quantum Heisenberg ferromagnetic with the nearest-neighbour interaction, described by the Hamiltonian:

$$H = -J \sum_{\langle ij \rangle} S_i \cdot S_j \tag{1.1}$$

with conventional notation.

In section 2 we only outline the essential features of the Handscomb MC approach, while the practical implementation of the Monte Carlo method [4, 5] is described in detail in the Appendix.

In sections 3.1.1 and 3.2 we discuss the results of numerical simulations. Comparisons are made with spin-wave theory predictions for susceptibility and energy behaviour [7, 8], the high-temperature expansions [2, 6] and the results of works in which various Monte Carlo methods were used to study two-dimensional quantum Heisenberg systems [2, 9, 10].

In section 3.1.4 simulated susceptibility temperature dependence is discussed as providing insights into the experimentally observed two-dimensional quantum ferromagnetic systems in ^{3}He found in [3].

2. Handscomb Monte Carlo method

When using the Handscomb MC method we perform a random walk over the space consisting of sequences C_r of spin permutation operators P_{ij}. The relevant observables such as energy E, zero-field susceptibility χT, specific heat C_v and spin-correlation functions $\langle S_i S_j \rangle$ are calculated as MC averages of certain parameters either of the permutation operators sequence C_r or the permutational cycles to which it can be reduced.

For the internal energy the expression is:

$$E = -\langle r \rangle / \beta + NJ. \tag{2.1}$$

Where $\langle\ \rangle$ is the expectation value calculated as a MC average, r is the sequence length, N is number of spins in the system.

For the specific heat:

$$C_v/k = \langle r^2 \rangle - \langle r \rangle^2 - \langle r \rangle. \tag{2.2}$$

For the susceptibility:

$$\chi T = \left\langle \sum_{j=1}^{k(C_r)} a_j^2 \right\rangle \tag{2.3}$$

where $k(C_r)$ is the number of cycles that make up the permutation induced by the sequence C_r, and a_j is the length of the jth cycle.

The contribution of current permutation to the spin correlation function $\langle S_i S_j \rangle$ is equal to $3/4$ if the spins situated in the ith and jth sites belong to the same permutational cycle, and is equal to zero if not.

The statistical errors of the numerical simulation were estimated in the conventional way: we have divided the whole MC run into ten or so blocks and monitored the difference between the overall average and the block ones.

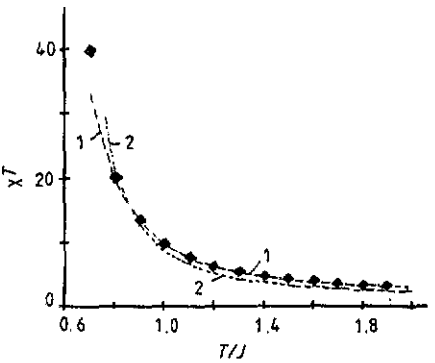

Figure 1. High-temperature susceptibility versus T/J, HT expansions fit: 1—quantum HTSE of [6]; 2—classical HTSE of [11], ◇—MC simulated susceptibility.

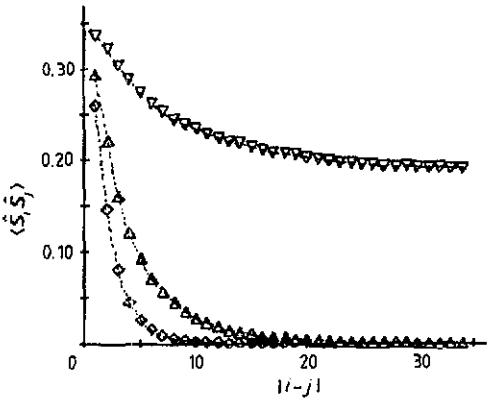

Figure 2. Spin-correlation functions for various temperatures. ▽—$L = 70$, $T/J = 0.3$; △—$L = 70$, $T/J = 0.7$; ◇—$L = 40$, $T/J = 1.0$.

3. Numerical simulation: results and discussion

The temperatures studied in the present work were situated mostly in the range $0.3 \leqslant T/J \leqslant 4.0$ (with the steps equal to 0.1). Lattice sizes varied from 16×16 to 80×80 sites for the lowest temperatures. Periodic boundary conditions were used everywhere. Markov chain lengths were approximately 1000 MCS spin^{-1} and the thermalization region length increased from 5000 MCS for the high temperatures to 1 500 000 MCS for the low temperatures.

Current values of energy and susceptibility were calculated every MCS, the spin-correlation functions were evaluated every 10 000 MCS.

3.1. Susceptibility

3.1.1. High-temperature region. The comparison was made between our simulated data and the high-temperature series expansion (HTSE) for susceptibility of the quantum [6] and the classical [11] models. As can be seen from figure 1 the simulation results and quantum HTSE are in a very good agreement for temperatures $T \geqslant 0.8J$, while there are small but systematic discrepancies in the case of classical HTSE in the temperature range $0.8 \leqslant T/J \leqslant 1.8$. Both expansions and numerical results merge as they approach unity with a further temperature increase.

Our study of the Padé approximations for the quantum susceptibility series failed to reveal (as opposed to Stanley's results for the classical susceptibility in [11]) the existence of non-zero critical temperature.

The same conclusion with regard to the quantum ferromagnetics was reached in [12], where the renormalization group approach was used to study quantum Heisenberg magnetics.

3.1.2. Extrapolation to infinite systems. Earlier works devoted to numerical simulations of a similar nature [2, 9] have not studied the size dependence of the susceptibility for various temperatures. This was mostly due to the still-high temperatures used in the

Table 1. Internal energy versus T/J for the various lattice sizes L, comparison with the Takahashi [7] spin-wave theory predictions.

T/J	$L = 24$	$L = 40$	$L = 50$	$L = 60$	[7]
0.3	0.975	0.958	0.974	0.968	0.9763
0.4	0.966	0.949	0.968	0.960	0.9571
0.5	0.947	0.921	0.946	0.926	0.9326
0.6	0.918	0.923	0.920	0.900	0.9025
0.7	0.888	0.875			0.8665
0.8	0.837	0.824			0.8247

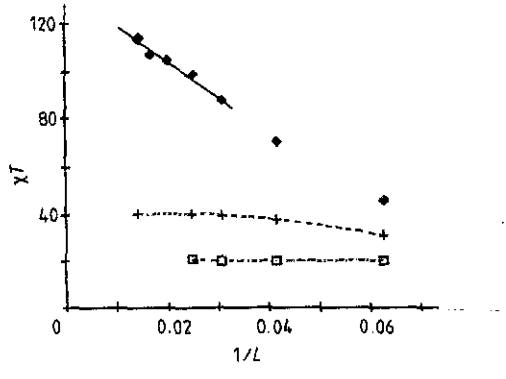

Figure 3. Finite-size effects for susceptibility: □—$T = 0.8J$, +—$T = 0.7J$, ◇—$T = 0.6J$.

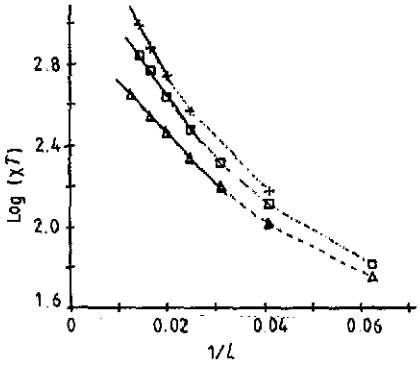

Figure 4. Finite-size effects for susceptibility. Susceptibility logarithm versus $1/L$: △—$T = 0.5J$, □—$T = 0.4J$, +—$T = 0.3J$.

simulations. As a result, the low-temperature susceptibility data in references [2, 9] tend to become unreliable even when presented in the papers.

Our calculations show that while internal energy is practically size-independent even at the lowest temperature $T/J = 0.3$ (see table 1 of section 3.2), the susceptibility does display a size dependence for the temperatures $T/J \leq 0.7$, owing to the dramatic growth of the correlation length with decreasing temperature (see figure 2).

The detailed analysis of the temperature–size dependence of the susceptibility showed that the behaviour conformed to the conventional scaling laws: when the size of the system is sufficiently large the properties of the system will become functions of its linear size L. The following equation was proposed for the staggered susceptibility in [1] where the numerical calculations were performed for two-dimensional quantum Heisenberg ferromagnetics:

$$\chi/TL^2 = f(\xi/L) \tag{3.1}$$

where ξ is the correlation length.

As can be seen in figure 3, when the temperature is equal to $0.6J$, our susceptibility for the larger systems is a linear function of inverse lattice size L. We have plotted on figure 4 the susceptibilities for the temperatures $0.3 \leq T/J \leq 0.5$ on the logarithmic scale. It is clear that the logarithms are the linear functions of $1/L$ (e.g. the plot for $T =$

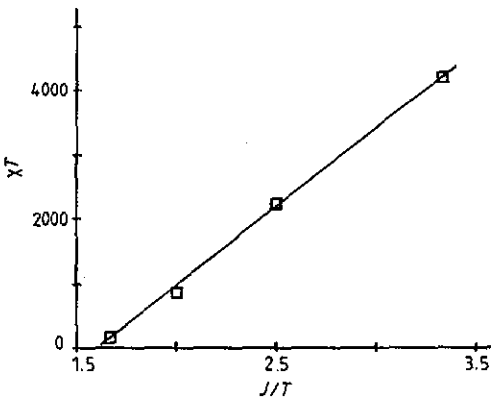

Figure 5. Susceptibility versus J/T for low temperatures (linear fit).

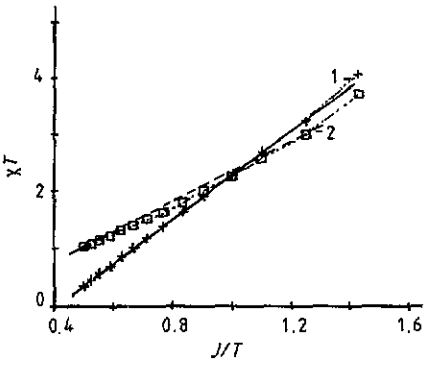

Figure 6. Susceptibility fit for spin-wave theories: + is $\log(\chi)$ versus J/T, full curve 1 ($\log\chi$) is the fit corresponding to [8]: $\chi = a\exp(8\pi bJ/T)$, □ is $\log(\chi T)$ versus J/T, broken curve 2 ($\log(\chi T)$) is the fit according to [7]: $\chi = (a_1/T)\exp(8\pi b_1 J//T)$.

0.5 J: five points from $L = 32$ to $L = 80$). We came to the conclusion that $f(\xi/L)$ has the form $c(T)\exp(-C\xi/L)$ where $c(T)$ is the infinite system susceptibility and C is a constant close to unity.

3.1.3. Comparison with the spin-wave theories. Extrapolation results of the previous section gave us a chance to compare the numerical simulation results for susceptibility with the low-temperature theoretical predictions. To be more specific, there have been proposed, from different spin-wave approaches [7, 8], the following equations for low-temperature susceptibility and correlation length as functions of temperature:

$$\chi = (a/T^l)\exp(8\pi bJ/T) \tag{3.2}$$

$$\xi = (a'/T^l)\exp(4\pi bJ/T) \tag{3.3}$$

with the Takahashi theory [8] giving $l = 0$, $b = 1/4$, $a = 1/3\pi J$, the Yamaji and Kondo theory [7] predicting $l = 1$ and $b = 1/8$ (for the 1/2 spin).

It is a common enough belief (see [2, 13]) that the existence of quantum fluctuations in the system will reduce the value of b compared with its theoretically predicted value.

The behaviour of the correlation length studied in [2] was found to fit quite well the following equation for temperatures $T'/J = 0.4$–5.0 (corresponding to our temperature range $T/J = 0.8$–10.0):

$$\xi = (a''/T'^{l})\exp(2\pi b'J/T'). \tag{3.4}$$

According to [2] the least squares fit yielded $l = 0$ and $b' = 0.172$, $a'' = 0.281$. It is interesting to note that in the same temperature range the correlation function of [2] is in good agreement with the HT approximation of [2].

$$\xi = 1/\ln(4J/T). \tag{3.5}$$

Our numerical simulations show (figure 5) that for $T/J = 0.8$–2.2 ($T'/J = 0.4$–1.1 of [2]) the susceptibility is described remarkably well by (3.2) with the parameters $l = 0$, $b = 0.151$ and $a = 0.211$ (full line), i.e. $\chi = a\exp(8\pi bJ/T)$. The dashed line of figure 6

is $\chi = (a_1/T)\exp(8\pi b_1 J/T)$, i.e. (3.2) with $l = 1$, and it is obviously a much poorer fit. When making comparisons between our fit for the susceptibility and that of [2] for the correlation length one has also to bear in mind the differences in temperature units between our work and [2]. Since (3.2) and (3.3) of the spin-wave theory suggest $\chi \sim \xi^2$ we were able to come to a conclusion that our results for the b parameter and those of reference [2] (b') are in a sufficiently good agreement ($b = 0.151$ and $b' = 0.172$).

The values of b in both cases are less than predicted by spin–wave theory, which may be due to the influence of quantum fluctuations as suggested in [2, 13].

It is instructive to note another similarity between our work and [2]: as in the case for correlation length, our data for susceptibility for $T/J = 0.8$–2.0 fit both HTSE (see figure 1 and section 3.1.1) and the low-temperature spin-wave approximation (namely, the Takahashi approach).

We have estimated the infinite-system susceptibilities for the temperatures $T/J = 0.3$–0.7 not available in the previous works [1, 2, 9, 11] and we came to a conclusion that for temperatures $T/J \leq 0.8$ it is impossible to describe the behaviour of the susceptibility by (3.2): it is obvious that χT diverges much slower than the exponential function. As it can be seen in figure 6, the discrepancies begin at temperature $T = 0.7J$ and cannot be accounted for by possible extrapolation errors, since figure 3 proves that for temperatures $T/J = 0.7$ and 0.8 we have already reached macroscopic values using the larger system sizes ($L = 40, 50, 60$).

It is easy to see (figure 5) that for $T/J = 0.3$–0.6 the susceptibility χT is a linear function of J/T.

$$\chi T = c + d/T \tag{3.6}$$

with the parameters extracted by the least squares fit being $c = 3986$ and $d = 2457$. Equation (3.6) means that for the lowest temperatures the susceptibility proper diverges as $T^{-\gamma}$, with the exponent γ very close to 2. It resembles the case of linear chains [14]. The possible existence of that kind of divergence for staggered susceptibility is discussed in [13], where the two-dimensional quantum Heisenberg antiferromagnetics were studied by the alternative Suzuki Monte Carlo method.

3.1.4. Comparison with the experimental data. The existence of the two-dimensional quantum ferromagnetism in thin films (2.5 layers) of ^{3}He on grafoil substrate was reported by Godfrin *et al* in [3] for the temperatures 10.0–0.7 mK. According to [3] the interaction in ^{3}He can be described by the quantum isotropic Heisenberg ferromagnetic Hamiltonian of (1.1) with the exchange constant $J = 2.1$ mK. Since the universal temperature corresponds to the range $0.3 < T/J < 5.0$ it is possible to compare the results of our numerical simulations and experimental data both at high- and low-temperature regions.

The comparison showed several distinctly similar features in the susceptibility behaviour. As was proved in section 3.1.1 the model susceptibility and the HTSE agree completely for $T/J > 0.8$. On the other hand, at the same range of temperatures our susceptibility follows quite well (see section 3.1.3) the exponential curve predicted by spin-wave theory. This peculiarity is closely parallelled by the behaviour of the experimental susceptibility of [3].

The experimental susceptibility at low temperatures ($0.3 < T/J < 0.9$) is a linear function of inverse temperature. Although the authors of [3] tend to blame this behaviour on saturation of the sample magnetization in non-zero magnetic fields, it is a feasible suggestion that in some range of temperature below $T/J = 0.9$, the power divergence

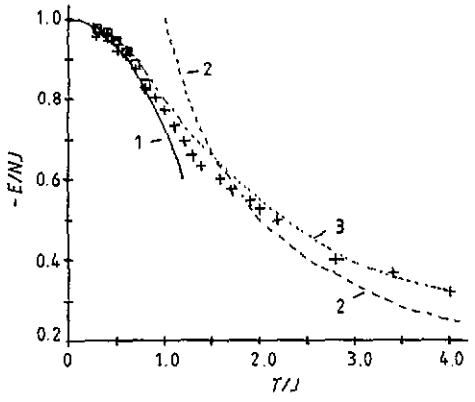

Figure 7. Internal energy versus T/J, our results: +—$L = 40$, □—$L = 24$, △—$L = 60$; 1—Takahashi low-temperature expansion of [6]; 2—high-temperature approximation of [2]; 3—results of [10] (Suzuki MC approach).

law reflects the essential trait of low-temperature behaviour of the two-dimensional quantum Heisenberg magnetics susceptibility.

3.2. Internal energy

In table 1 we present the internal energy values for various temperatures T and system sizes L. One can see that the differences in the energy values for the same temperatures do not display any systematic trend; they are not the monotonous functions of the lattice size and they agree within the error bars (2–3%).

The comparison between our results, various theoretical approximations and the other numerical experiments can be seen in figure 7. We have plotted there: (1) our results; (2) the results of [10] where the energy of the quantum Heisenberg magnetics is studied with the Suzuki Monte Carlo method; (3) the high-temperature approximation, proposed in [2]; and (4) the low-temperature expansion derived from the Takahashi spin-wave theory [8, 10]:

$$E = -1 + (\zeta(2) + \zeta(3)T/4)T^2/2\pi \tag{3.7}$$

where ζ is the zeta-function and E and T are expressed in units of exchange constant J.

The results of [9] follow the expansion (3.7) only up to the temperature $T = 0.4J$, while our results agree well with (3.7) for temperatures $T/J < 0.9$.

The specific heat peak is situated (for both simulations) somewhere in the region of $0.85 < T/J < 0.95$ that is, right at the point where the discrepancies with the theory begin to appear.

As the theoretical curve for the energy does not contain the inflection necessary for the existence of a specific heat peak point, it is highly probable that 0.85–$0.95J$ are the temperatures that limit the applicability of the Takahashi theory.

For temperatures higher than $T = 3.0J$ our results and those of [10] begin to agree once again, while disagreeing dramatically with the [2] approximation. According to [2] product ET will tend to become constant with increasing temperature. Our results show that this is not true even for the highest temperatures used ($T/J = 9.6$ and 20) when the susceptibility of the system is close to unity.

4. Summary

We have calculated in the present work the equilibrium properties (susceptibility, internal energy and specific heat) of the quantum two-dimensional Heisenberg ferromagnetic system with the nearest-neighbours interaction.

The Handscomb quantum Monte Carlo approach was used. The large system sizes we used in the simulations made it possible for us to apply a scaling method and to achieve reliable results for the infinite system susceptibility in a temperature range considerably lower than those studied elsewhere.

We have also checked our results for the susceptibility and energy against those of other numerical experiments and various theoretical predictions. The comparisons have enabled us to define temperature regions where the high- and low-temperature approximations are valid (if they are at all, as in the case of the HTA for energy). The results of the numerical simulations can also be used to fill the gap between the HT and LT approximations.

Appendix

It is a matter of common knowledge that a straightforward application of the Monte Carlo method is impossible in the case of quantum systems. The first attempt to overcome the difficulties arising from the non-commutativity of spin operators in the quantum Heisenberg Hamiltonian

$$\boldsymbol{H} = -2\mu H \sum_{i=1}^{N} \boldsymbol{S}_i - 2J \sum_{i=1}^{N_b} \boldsymbol{S}_{l(i)} \cdot \boldsymbol{S}_{l'(i)} = \boldsymbol{H}_0 + \sum_{i=1}^{N_b} \boldsymbol{H}(i) \tag{A1}$$

was made by Handscomb in [4] and the approach was developed further by Lyklema [5]. (N is number of spins, N_b is number of bonds, H is transverse magnetic field.)

Since operator $\boldsymbol{H}_0$ and each of the $\boldsymbol{H}(i)$ operators do commute we can expand only $\exp\{-\beta\Sigma\boldsymbol{H}(i)\}$ in a two-fold sum: a series over the inverse temperature multiplied by a sum corresponding to

$$\left\{\sum_i \boldsymbol{H}(i)\right\}^r = \sum_{C_r} \boldsymbol{H}(i_1)\boldsymbol{H}(i_2)\ldots\boldsymbol{H}(i_r) \tag{A2}$$

where Σ_{C_r} is the sum over all possible combinations of sequences C_r of operators: $C_r = i_1, i_2 \ldots i_r$, i_k is an arbitrary bond number. The partition function Z can be written as:

$$Z = \mathrm{Tr}\{\exp(-\beta\boldsymbol{H})\} = \mathrm{Tr}\left\{\exp(-\beta\boldsymbol{H}_0) \sum_{r=0}^{\infty} [(-\beta)^r/r!] \sum_{C_r} \boldsymbol{H}(i_1)\boldsymbol{H}(i_2)\ldots\boldsymbol{H}(i_r)\right\}. \tag{A3}$$

If we also interchange the orders of trace and summations operations it will be possible to estimate the average of any observable A as the expectation value of a certain variable (estimator) Ω_A defined in the space consisting of all the possible sequences (strings) of operators C_r:

$$\Omega_A(C_r) = \frac{\mathrm{Tr}\{\boldsymbol{A}\boldsymbol{H}(i_1)\boldsymbol{H}(i_2)\ldots\boldsymbol{H}(i_r)\exp(-\beta\boldsymbol{H}_0)\}}{\mathrm{Tr}\{\boldsymbol{H}(i_1)\boldsymbol{H}(i_2)\ldots\boldsymbol{H}(i_r)\exp(-\beta\boldsymbol{H}_0)\}} \tag{A4}$$

To establish the Markov walk one has to define weights of elements. In order to do

this we use the well-known operator identity involving spin-1/2 operators $S_t S_{t'}$ and permutation operator $E(t, t')$:

$$E(t, t') = (4S_t S_{t'} + 1)/2. \tag{A5}$$

Permutation operator $E(t, t')$ interchanges the spin eigenvalues, i.e. it switches the spins currently situated in the t and t' sites of the lattice.

If we introduce $\pi(C_r)$ as

$$\pi(C_r) = [(-\beta)^r/r!]\mathrm{Tr}\{\boldsymbol{H}(i_1)\boldsymbol{H}(i_2)\ldots\boldsymbol{H}(i_r)\,\mathrm{e}^{-\beta H_0}\}$$

then in the ferromagnetic case, when $\boldsymbol{H}(i) = -JE(t_i, t_i')$

$$\pi(C_r) = [(\beta J)^r/r!]\,\mathrm{Tr}\left\{\prod_{i_k=1}^{r} E(t(i_k), t'(i_k))\right\} = (\beta J)^r/r!\prod_{j=1}^{k(C_r)} 2\cosh(\mu\beta H a_j/2kT) \geqslant 0 \tag{A6}$$

where $k(C_r)$ is the number of cyclic permutations (cycles) to which sequence C_r can be reduced; a_j is length of the jth cycle.

We can, further, write Z as the sum over $\pi(C_r)$

$$Z = \sum_{r=0}^{\infty}\sum_{C_r}\pi(C_r) \tag{A7}$$

$$p(C_r) = \pi(C_r)/\sum\sum\pi(C_r) \geqslant 0. \tag{A8}$$

Obviously $p(C_r)$ is the normalized probability of the C_r element. The average of any given operator A is the expectation value of the Ω_A estimator and can be estimated using the conventional Monte Carlo technique described below.

$$\langle A\rangle = \sum_{r=0}^{\infty}\sum_{C_r}\Omega(C_r)p(C_r) = \varepsilon\{\Omega(C_r)\}. \tag{A9}$$

A.1. Monte Carlo steps

During the random walk over operator sequences space we perform three kinds of steps.

(i) *Direct step.* We add one randomly selected permutation operator to the end of the current sequence C_r

$$C_{r+1}' = i_1 i_2 \ldots i_r i_{r+1}. \tag{A10}$$

(ii) *Reverse step.* We delete the first operator from the sequence

$$C_{r-1}'' = i_2 i_3 \ldots i_r. \tag{A11}$$

(iii) *Cyclic permutation.* Since the cyclic permutation does not change the outcome of trace operation it was suggested by Handscomb when one of the steps was rejected to perform a cyclic permutation in the string C_r

$$C_r''' = i_r i_1 \ldots i_{r-1}. \tag{A12}$$

A.2. Program storage structure

We used the following arrays in our program:

(i) CR—integer array where the string of indices defining C_r sequence 'floats'; the current boundaries of the sequence are integer markers INDI1 and INDIR.

(ii) PCR—integer array containing the information about current spin permutation: PCR(I) = index of the spin situated right now in the ith site of the lattice.

(iii) PRC—integer array: PRC(I) = location of that site where the ith spin is situated.

(iv) LC—integer array: if LC(I) = LC(K) the spins in the ith and kth sites belong to the same cyclic permutation, otherwise they do not.

(v) ICY—the array where information concerning the lengths of all the cycles is stored.

A.3. Step probabilities and acceptance ratios

According to Lyklema the direct step probability P can be written as:

$$P(C_r \rightarrow C_{r+1}) = f_r p_i T^+(C_r \rightarrow C_{r+1}) \tag{A13}$$

where f_r is the probability of selecting a direct step, p_i the probability that we select the given permutation, $T^+(C_r \rightarrow C_{r+1})$ the direct step acceptance ratio.

The probability of the reverse step is

$$P(C_{r+1} \rightarrow C_r) = (1 - f_r)T^-(C_{r+1} \rightarrow C_r) \tag{A14}$$

where $T^-(C_{r+1} \rightarrow C_r)$ is the reverse step acceptance ratio. The detailed balance principle requires

$$p(C_r)P(C_r \rightarrow C_{r+1}) = p(C_{r+1})P(C_{r+1} \rightarrow C_r) \tag{A15}$$

taking into account (A4) we can write

$$\pi(C_r)P(C_r \rightarrow C_{r+1}) = \pi(C_{r+1})P(C_{r+1} \rightarrow C_r). \tag{A16}$$

It is easy to see that (A15) will be satisfied if T^+ and T^- functions have the following form:

$$T^+(C_r \rightarrow C_{r+1}) = \min\{1, (1 - f_{r+1})p(C_{r+1})/p_i' f_r p(C_r)\} \tag{A17a}$$

$$T^-(C_{r+1} \rightarrow C_r) = \min\{1, p_{i+r} p(C_r)/(1 - f_{r+1})p(C_{r+1})\}. \tag{A17b}$$

A.4. Monte Carlo steps realization

A.4.1. Direct step

We select the direct step with the probability f_r (or the reverse step with the probability $1 - f_r$)

$$f_0 = 1 \qquad f_r = 1/2 \qquad r = 1, 2, 3 \ldots$$

the permutation operator $E(T, T1)$ is selected with the probability $1/N_b$. We already know (LC array) whether the spins in T and $T1$ sites belong to the same cycle or not and

can estimate the acceptance ratio T^+ of the step. Then depending on the T^+ value we either add the permutation operator to the end of the C_r string (see A10) or have to reject the step (if $T^+ < \xi < 1$ where ξ is a random number generated when $T^+ < 1$).

A.4.2. Reverse step

Since $E(t, t')E(t, t') =$ unity operator, we have to apply the permutation operator $E(t_{i_1}, t'_{i_1})$ to the beginning of the string C_r in order to delete the first operator:

$$C''_{r-1} = i_1 i_1 i_2 \ldots i_r = i_2 i_3 \ldots i_r. \tag{A18}$$

The difference between the forward and reverse steps is the following: during the forward step we add the permutation to the end of the string and it results in a switching of spins currently situated in the T and $T1$ sites corresponding to the selected bond (information stored in the PCR array). When performing a reverse step we add the permutation to the beginning of the string and we have to exchange the T and $T1$ spins themselves. Information about their present positions is stored in a PRC array (of course, after the steps are performed we update both PCR and PRC arrays).

The similarity between the steps allows us to deal with acceptance ratios in terms of permutation cycles only:

$$\frac{\pi(C_{r+1})}{\pi(C_r)} = \frac{\beta J}{r+1} \times \begin{cases} 2 & \text{if } A \\ 1/2 & \text{if } B \end{cases} \tag{A19a}$$

$$\frac{\pi(C_{r-1})}{\pi(C_r)} = \frac{r}{\beta J} \times \begin{cases} 2 & \text{if } A \\ 1/2 & \text{if } B \end{cases} \tag{A19b}$$

where A is the case when the spins belonged to same cycle, and B where the spins belonged to different cycles.

One has also to keep track of the cycles by updating the LC array. If two spins belonged to different cycles the application of the spin permutation merges the cycles and the knowledge about the lengths of the cycles (array ICY) allows us to rename the shorter cycle.

If the exchanged spins belonged to the same cycle, this is split and after the permutation we have two cycles. It is impossible to say beforehand which will be the shorter. In this case we walk over the PCR array to define the elements belonging to one of the cycles. Still, measuring the cycle length and updating the LC array will take place for one only of the two new cycles.

A.4.3. Cyclic permutation

In order to simplify the program we performed cyclic permutation only when the reverse step had been rejected. All the pertinent information was at hand already. Alterations included only the pair exchanges in PCR, PRC, CR and LC arrays and did not call for the walk over PCR array or lengthy updating in the LC array.

References

[1] Gomes-Santos G and Joannopoulos J D 1989 *Phys. Rev.* B **39** 4435–51

[2] Manousakis E and Salvador R 1989 *Phys. Rev.* B **39** 575–85
[3] Godfrin H, Ruel R R and Osheroff D D 1988 *Phys. Rev. Lett.* **60** 305–308
[4] Handscomb D C 1964 *Proc. Camb. Phil. Soc.* **60** 115–30; 1962 *Proc. Camb. Phil. Soc.* **58** 594–609
[5] Lyklema J W 1982 *Phys. Rev. Lett.* **49** 88–92
[6] Baker G A, Gilbert H E, Eve J and Rushbrooke G S 1967 *Phys. Lett.* **25A** 207–9
[7] Yamaji K and Kondo J 1973 *Phys. Lett.* **45A** 317–22
[8] Takahashi M 1986 *Prog. Theor. Phys. Suppl.* **87** 233–44
[9] Chakravarti S and Stein D B 1982 *Phys. Rev. Lett.* **49** 582–5
[10] Okabe J and Kibuchi M 1988 *J. Phys. Soc. Japan* **57** 4351–6
[11] Stanley N E 1967 *Phys. Rev.* **158** 546–58
[12] Drzewiski A and Sznajd J 1988 *Phys. Lett.* **60** 840–3
[13] Miyashita S 1988 *J. Phys. Soc. Japan* **57** 1934–45
[14] Chen Y C, Chen H H and Lee F 1988 *Phys. Lett.* **130A** 257–9